

**Electronic structure of the indium-adsorbed Au/Si(111)- $\sqrt{3} \times \sqrt{3}$  surface: A first-principles study**Chia-Hsiu Hsu,<sup>1</sup> Wen-Huan Lin,<sup>1</sup> Vidvuds Ozolins,<sup>2</sup> and Feng-Chuan Chuang<sup>1,2,\*</sup><sup>1</sup>*Department of Physics, National Sun Yat-sen University, Kaohsiung 804, Taiwan*<sup>2</sup>*Department of Materials Science and Engineering, University of California, Los Angeles, California 90095-1595, USA*

(Received 27 October 2011; revised manuscript received 12 March 2012; published 2 April 2012)

Electronic structures of the indium-adsorbed Au/Si(111)- $\sqrt{3} \times \sqrt{3}$  surface were examined using first-principles calculations at In coverages of 0, 1/6, 1/3, 2/3, and 1 ML. The band structures of the numerous models were analyzed in detail. We found that the surface bands around the  $M$  point exhibit notable Rashba-type spin-orbit splittings. In addition, our results show that the calculated bands of the lowest-energy model at 1/3 ML are in fair agreement with the identified bands in the angle-resolved photoemission study [J. K. Kim *et al.*, *Phys. Rev. B* **80**, 075312 (2009)].

DOI: 10.1103/PhysRevB.85.155401

PACS number(s): 68.35.B-, 68.43.Bc, 73.20.At

**I. INTRODUCTION**

Metal overlayers on a semiconductor surface have generated huge research interest in recent years due to their low-dimensional electronic properties and potential applications in the microelectronics industry. One of the prototypical systems under intensive study is the Au overlayers on the Si(111) surface.<sup>1–40</sup> Depending on the Au coverages and the annealing conditions, the Au/Si(111) system exhibits various surface reconstructions, such as  $5 \times 1$ ,  $5 \times 2$ ,  $\sqrt{3} \times \sqrt{3}$ ,  $6 \times 6$ , etc.<sup>1–40</sup>

Depending on the orientation of the reconstruction, a surface exhibits either two-dimensional (2D)<sup>20,40–43</sup> or one-dimensional (1D) metallic characteristics.<sup>34</sup> Recent studies have shown that the complex surface band structure of the Pb/Si(111)- $\sqrt{7} \times \sqrt{3}$  phase is governed by a simple 2D free-electron character,<sup>20,40–43</sup> while the Au/Si(111)- $5 \times 2$  phase exhibits a 1D feature.<sup>18,30</sup>

The  $\sqrt{3} \times \sqrt{3}$  ( $\sqrt{3}$  hereafter) phase of Au/Si(111) has been studied extensively,<sup>1–21</sup> and the well-known conjugate honeycomb-chained-trimer (CHCT) model<sup>10,12,21,44,45</sup> for  $\sqrt{3}$  is regarded as the lowest-energy model at Au coverage of 1 ML. The previous calculated band structure of this model is in fair agreement with the angle-resolved photoelectron spectroscopy (ARPES).<sup>45</sup> However, there is a small discrepancy between the experimental data reported by Zhang *et al.*<sup>19</sup> and Altmann *et al.*<sup>18</sup> Both studies showed that the two bands  $S_2$  and  $S_3$  are degenerate at the  $\Gamma$  point. While the results of Zhang *et al.*<sup>19</sup> seem to indicate that  $S_2$  and  $S_3$  bands do not merge and leave a band opening of around 0.4 eV at the  $M$  point, Altmann *et al.*<sup>18</sup> found that these bands do in fact merge at the  $M$  point, at least within an uncertainty of about 0.1 eV imposed by the lifetime broadening.

Recently, there has been a slew of very interesting reports concerning domain walls of the  $\sqrt{3}$ -Au surface.<sup>46–48</sup> The scanning-tunneling-microscopy (STM) study<sup>46</sup> found that submonolayer In adsorbates (0.15–0.4 ML) on the  $\alpha$ - $\sqrt{3}$ -Au surface eliminate the whole domain wall to yield a very well ordered and homogeneous  $\sqrt{3} \times \sqrt{3}$  ( $h$ - $\sqrt{3}$  hereafter) phase. More recently, Kim *et al.*<sup>48</sup> measured the surface band dispersions and Fermi surfaces before and after the In adsorption on the Au/Si(111)- $\sqrt{3}$  using ARPES. They found that In adsorbates do not significantly alter the surface band

structure but shift the bands by about 200–500 meV. Moreover, result from core-level photoelectron spectroscopy by Kim *et al.*<sup>48</sup> suggested that In adsorbates interact directly with the surface Si atoms rather than Au atoms. Thus, it is highly likely that the In atoms adsorb in the middle of the Si trimers, as suggested by the STM study.<sup>46</sup>

Moreover, strong Rashba-type spin-orbit splittings in the surface alloy on Si(111) and Ge(111) have attracted some research interest.<sup>49–52</sup> In view of these experimental data for the In-adsorbed Au/Si(111)- $\sqrt{3}$  phase, a further theoretical study is required in order to clarify the adsorption structure of In atoms and to further check the effect of In adsorbates on the surface band dispersion, as well as to examine whether this surface alloy will produce strong Rashba-type spin-orbit splittings.

In this paper, we examined the atomic and electronic structures of the indium-adsorbed Au/Si(111)- $\sqrt{3}$  surface using first-principles calculations. For some adsorption sites and structural motifs, the surface band structures do not change dramatically. Instead, the whole band structures were shifted by  $-329$  to  $850$  meV. We found that the surface bands around the  $M$  point exhibit notable Rashba-type spin-orbit splittings. The calculated bands for the lowest-energy model at In coverage of 1/3 ML are in fair agreement with the identified bands in the angle-resolved photoemission study.<sup>48</sup> The surface band dispersion of the lowest-energy structures at indium coverage of 2/3 ML is quite interesting and may have further implications.

The rest of this paper is arranged as follows: In Sec. II, the computational methods are discussed. Results and discussion of atomic and calculated band structures are presented in Sec. III. Finally, our major findings in this work are summarized with a brief conclusion in Sec. IV.

**II. COMPUTATIONAL METHODS AND STRUCTURAL MODELS**

The calculations were carried out within the generalized gradient approximation<sup>53</sup> to density functional theory<sup>54</sup> using projector-augmented-wave potentials,<sup>55</sup> as implemented in Vienna Ab-Initio Simulation Package.<sup>56</sup> The kinetic energy cutoff was set to 500 eV (36.75 Ry), and the gamma-centered  $10 \times 10 \times 1$  Monkhorst-Pack grid was used to sample the

TABLE I. The relative surface energies  $\Delta E_s$  (meV per  $\sqrt{3}$  cell) with respect to the CHCT model of proposed models.  $E_{\text{shift}}$  is the energy shift (meV) of ARPES data to match our calculated band structures.  $\delta E_o$  (meV) is the band opening at the  $M$  point with SOC. The values in the parentheses are without SOC.

Label	Figure	$\theta_{\text{In}}$	$\theta_{\text{Au}}$	$\theta_{\text{Si}}$	$\Delta E_s$ (meV per $\sqrt{3}$ )	$E_{\text{shift}}$ (meV)	$\delta E_o$ (meV)
CHCT	1(a)	0	1	1	0	+ 250	258(311)
HCT	1(b)	0	1	1	83		
CHCT-T4		1/6	1	1	- 149		
CHCT-AT		1/6	1	1	- 12		
CHCT-AS		1/6	1	1	22		
Substitute <sup>a</sup>		1/6	5/6	1	434		
Distorted substitute <sup>b</sup>		1/6	1	5/6	754		
CHCT-T4	1(c)	1/3	1	1	- 183	-100	261 (354)
CHCT-AT	1(d)	1/3	1	1	231	-329	170 (212)
CHCT-AS		1/3	1	1	243		
Distorted substitute <sup>b</sup>	2(a)	1/3	1	2/3	352		
Substitute <sup>a</sup>	2(b)	1/3	1	2/3	433	+ 850	133(79)
Distorted substitute <sup>b</sup>	2(c)	1/3	2/3	1	599		
CHCT-2T4	3(a)	2/3	1	1	7		
CHCT-1T4-1AT	3(b)	2/3	1	1	215		
CHCT-2AS	3(c)	2/3	1	1	444		
CHCT-1AT-1AS	3(d)	2/3	1	1	579	-300	118 (159)
Distorted substitute <sup>b</sup>		2/3	2/3	1	555		
Distorted substitute <sup>b</sup>		2/3	1	2/3	215		
CHCT-2T4-1AT		1	1	1	172		
CHCT-3AS		1	1	1	303		

<sup>a</sup>The CHCT motif is retained after In substitution.

<sup>b</sup>The CHCT motif is not retained after In substitution.

surface Brillouin zones (SBZ) for the  $\sqrt{3}$  phases. Moreover, for all our surface calculations, the theoretical Si bulk lattice constant of 5.468 Å was adopted. We employed a periodically repeating slab consisting of three Si bilayers, a reconstructed layer, and a vacuum space of  $\sim 12$  Å. Hydrogen atoms were used to passivate the Si dangling bonds at the bottom of the slab, and the positions of H atoms were kept fixed. Similarly, the silicon atoms of the bottom bilayer were kept fixed at the bulk crystalline positions. The remaining In, Si, and Au atoms were relaxed until the residual force was smaller than 0.01 eV/Å.

After calculating the total energies of the models, the relative surface energy  $\Delta E_s$  with respect to the lowest-energy model, CHCT, of the  $\sqrt{3}$  phase at Au coverage of 1.0 ML is calculated next according to the relation

$$\Delta E_s = E_{\text{model}} - E_{\text{CHCT}} - \Delta\theta_{\text{In}}\mu_{\text{In}} - \Delta\theta_{\text{Si}}\mu_{\text{Si}} - \Delta\theta_{\text{Au}}\mu_{\text{Au}}. \quad (1)$$

In the above,  $E_{\text{CHCT}}$  and  $E_{\text{model}}$  are the total energies of the CHCT- $\sqrt{3}$  and the proposed models, respectively.  $\mu_{\text{In}}$ ,  $\mu_{\text{Au}}$ , and  $\mu_{\text{Si}}$  denote the chemical potentials of the bulk phases, and  $\Delta\theta_{\text{In}}$ ,  $\Delta\theta_{\text{Au}}$ , and  $\Delta\theta_{\text{Si}}$  represent the differences in coverages in the surface layer for the proposed models with respect to the CHCT model. The relative surface energies  $\Delta E_s$  of the models listed in Table I are calculated by setting the bulk energies of Au, Si, and In to the values of their respective chemical potentials. Both calculated band structures with and

without the spin-orbit coupling (SOC) for the representative models are shown in the figures.

Finally, we have manually created the atomic structures for various In coverages. In addition, we also randomly placed In, Au, and Si atoms on the substrate and then relaxed them to their local minima. In total, we examined roughly 30 structures for the In coverages of 1/3 and 2/3 ML. Of these, selected low-energy models are shown in Table I and Figs. 1–3.

### III. RESULTS AND DISCUSSION

The well-known conjugate honeycomb-chained-trimer model<sup>10,12,19,21,44,45</sup> for the  $\sqrt{3}$  phase is illustrated in Fig. 1(a), where Au atoms form the trimer. The corresponding band structure of the CHCT model is shown in Fig. 1(e). Our calculated band structure along  $\Gamma$ - $M$ - $\Gamma$  is similar to that reported by Lee and Kang.<sup>45</sup> The red dotted lines represent the ARPES data reproduced from Ref. 48. The experimental result is shifted by +250 meV in order to match the band merging feature at the  $M$  point. However, the experimental bands  $S_2$  and  $S_3$  merging at the  $M$  point is not replicated in the theoretical calculation. Rather, the band opening of 0.311 eV,  $\delta E_o$ , at the  $M$  point is observed. We further reexamined the band structures of the  $1 \times 1$  model shown in Fig. 1(a) of Ref. 48 and find that the degeneracy of  $S_2$  and  $S_3$  at the  $M$  point is broken by the trimerization of the Au atoms and result in a band gap of 0.311 eV at the  $M$  point. However, further spin-orbit coupling calculations result in splitting and broadening of  $S_2$  and  $S_3$  such

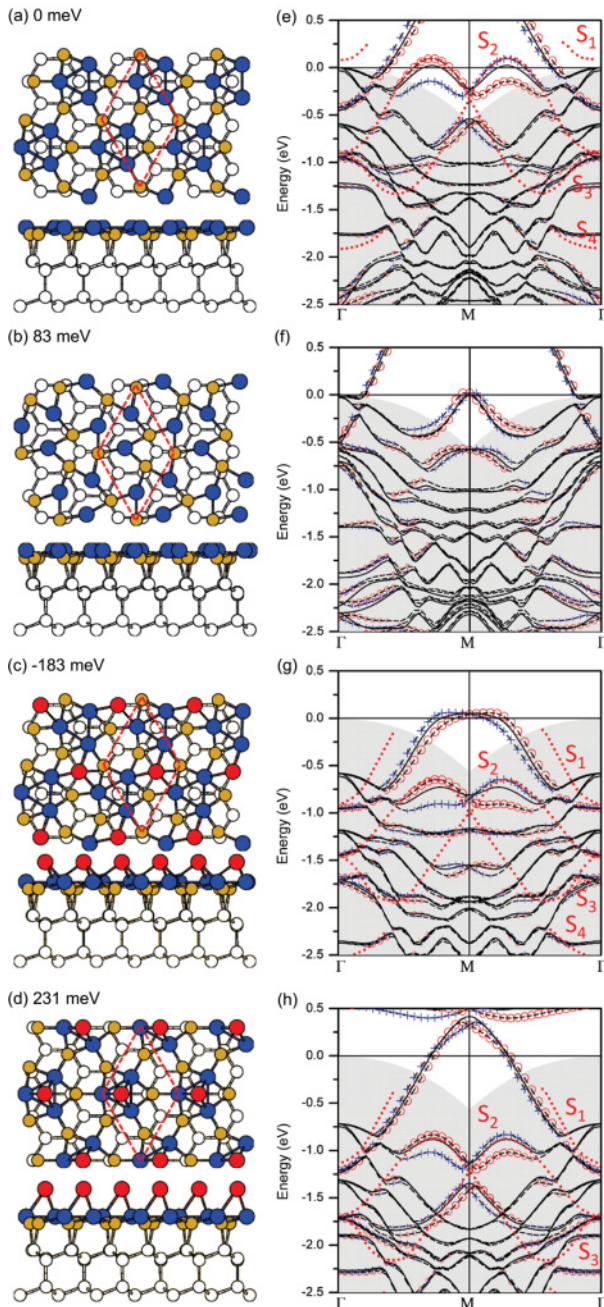


FIG. 1. (Color online) (a) and (b) show the optimized atomic structures for the  $\sqrt{3}$  phase, and (e) and (f) are their corresponding band structure along the  $\Gamma$ -M- $\Gamma$ . (c) and (d) show models for a single In atom adsorbed on  $\sqrt{3}$  corresponding to In coverage of 1/3 ML, while (g) and (h) are their corresponding band structures along the  $\Gamma$ -M- $\Gamma$ . The  $\sqrt{3}$  supercell is outlined with the red dashed lines. The values above the models are the relative surface energies (meV per  $\sqrt{3}$  cell) with respect to CHCT model. Large red (medium gray) and blue (dark gray) and small golden (light gray) filled circles indicate In, Au, and Si atoms of the surface layer, respectively, and white spheres represent Si atoms below the surface layers. For the band structures, the solid lines indicate the results without SOC. The red circles and blue crosses in the band structures indicate opposite spin orientations, and their sizes are proportional to contributions of the Au, In, and Si atoms at the surface layer. The dashed lines are the band structures including SOC. The red dotted lines are the ARPES data reproduced from Ref. 48.

that these  $S_2$  and  $S_3$  bands seem to be closer around the  $M$  point (a gap of 0.258 eV). The calculated highest surface band,  $S_1$ , differs from the experimental value by around 0.4 eV at the  $\Gamma$  point. Next, the honeycomb-chained-trimer (HCT) model shown in Fig. 1(b) is found to be higher in energy by 83 meV per  $\sqrt{3}$  where its band structure is shown in Fig. 1(f). Based on Fig. 1(f), it would seem that the band structure of the HCT model does not match the experimental result. Apparently, the band structure is sensitive to surface atomic reconstruction.

After reexamining the  $\sqrt{3}$  phase, we began to simulate the experimental studies<sup>46-48</sup> where the indium atoms were adsorbed on the  $\sqrt{3}$  surface. We started with a single indium atom per  $\sqrt{3}$  cell, which corresponds to a coverage of 1/3 ML. Numerous structures were examined, and first two lowest-energy are shown in Figs. 1(c) and 1(d). The model in Fig. 1(c) shows that the indium atom resides at a position higher than the Au atoms and is found among the Au trimers. Moreover, it bonds with the Au atoms of the three neighboring trimers. The position of this In atom is right on top of the T4 site with respect to the underlying Si(111) substrate. Thus, we label it as the CHCT-T4 model. The In position in the model shown in Fig. 1(c) is, in fact, the same as the site proposed by previous studies.<sup>46,48</sup> Furthermore, the model in Fig. 1(c) has a lower relative energy than the CHCT model. Nonetheless, the band structure in Fig. 1(g) is in fair agreement with the experimental observations.  $S_3$  is not fully replicated in the calculations. The second model shown in Fig. 1(d) shows the indium atom residing on top of the Au trimer. It was therefore appropriately labeled as the CHCT-AT model. The band structure of this CHCT-AT model at In coverage of 1/3 ML agrees well with the experimental band when shifted by  $-329$  meV, as shown in Fig. 1(h). The band dispersions of  $S_1$ ,  $S_2$ , and  $S_3$  match the experimental bands. In addition, our calculations with and without the SOC exhibit band openings of 212 and 170 meV at the  $M$  point, respectively. It appears that the In atoms behave as the electron donors when they reside on top of Au trimers. Finally, the possible adsorption site with the next higher energy is found to be on top of the Si atom and then is labeled CHCT-AS. The relative energy of this model is included in Table I. However, since its band structure does not match the experiment, we will not present it in this study.

We further explored other possibilities. In one possible scenario, the CHCT model is no longer retained after In adsorptions. Numerous models were then examined, and we illustrate two models wherein one Si atom is replaced by one In atom at In coverage of 1/3 ML, as shown in Figs. 2(a) and 2(b). For the first In substitution model, the CHCT is broken; thus the band structure in Fig. 2(d) does not match the experimental result. For the second In substitution model, the CHCT is retained after the Au atom was substituted by an In atom. The band structure of the second model shown in Fig. 2(e) reproduces the experimental  $S_2$  and  $S_3$  bands well, provided the experimental result is shifted by  $+850$  meV. The  $S_2$  and  $S_3$  bands differ by 0.079 and 0.133 eV around the  $M$  point, which is close to the experimental resolution limit of 0.1 eV.<sup>18</sup> Furthermore, we also explored the coverage where the Au atom is substituted by an In atom. One such model is shown in Fig. 2(c), where it appears that its band structures does not match the experimental observation.

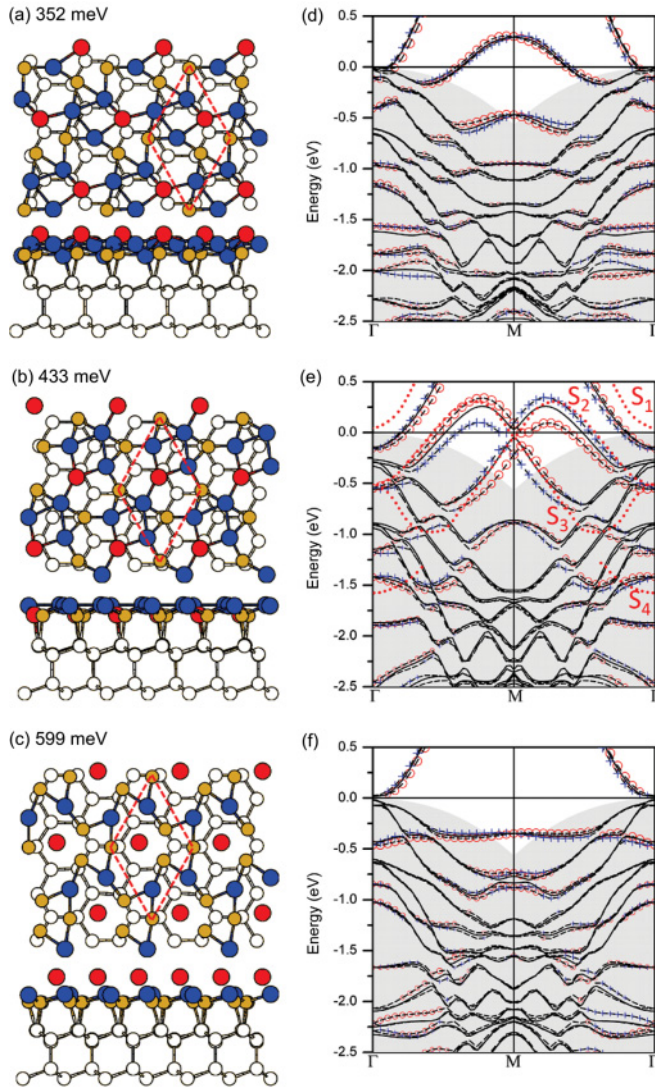


FIG. 2. (Color online) (a) and (b) show models at In coverage of  $1/3$  ML where one In atom substitutes the Si atom for each  $\sqrt{3}$  cell, and (d) and (e) are their corresponding band structures along the  $\Gamma$ - $M$ - $\Gamma$ . (c) depicts the model at In coverage of  $1/3$  ML where one In atom substitutes one Au atom at the surface layer, and its corresponding band structure is shown in (f).

In the experiment at around In coverage of  $0.15$  ML, a sharp  $\sqrt{3} \times \sqrt{3}$  low-energy electron diffraction (LEED) pattern without any other diffraction features developed.<sup>46,48</sup> Therefore, after determining the possible adsorption sites at  $1/3$  ML, we intuitively augmented our supercell to a  $2\sqrt{3} \times \sqrt{3}$  unit such that one In atom in the supercell corresponds to  $1/6$  ( $0.167$ ) ML, approximately close to the experimental coverage of  $0.15$  ML. Moreover, the other possible models are that ones in which an In atom substitute either one Au atom or a Si atom on the surface. We have examined three sites and numerous substitution models, and those with low energies are listed in Table I. Our result is in agreement with the previous calculation by Gruznev *et al.*<sup>46</sup> in which the CHCT-T4 model is the lowest-energy adsorption site. Since additional discussions of the CHCT-T4 models at  $1/6$  and  $1/3$  ML can be found in the aforementioned study,<sup>46</sup> we will not elaborate further here.

Furthermore, we also noted that the In atom substitution of a Si atom and a Au atom in the  $\sqrt{3}$  cell are energetically unfavorable, which also mirrors the experimental finding<sup>46</sup> that the Si coverage and the Au coverage were found to be  $1$  ML. The energies of the models at In coverage of  $1/6$  ML are higher than that of the lowest-energy model shown in Fig. 1(a) at In coverage of  $1/3$  ML.

The In coverage was increased to  $2/3$  ML so that two indium atoms are in a  $\sqrt{3}$  unit. Since we know the possible adsorption sites for the In atoms from the models with In coverage of  $1/3$  ML, these possible sites are enumerated to generate new structural models. In addition, an In atom also substitutes position of Au or Si atoms. Furthermore, we performed random arrangement of atoms on the surface. Up to 30 structures were examined, and four low-energy structural models are illustrated in Fig. 3. The model with the lowest energy in Fig. 3(a) has two indium atoms residing among the Au trimers in a way similar to the CHCT-T4 model in Fig. 1(a). This model is found to be identical to that illustrated by Kim *et al.*<sup>48</sup> We note that the models at  $1/6$  and  $1/3$  ML have lower energies than the model at In coverage of  $2/3$  ML. The band structure shown in Fig. 3(e) of the lowest-energy model at In coverage of  $2/3$  ML does not match the experimental result. However, the surface band dispersion of the lowest-energy structures at indium coverage of  $2/3$  ML is quite interesting and may have further implications. The second-lowest-energy model shown in Fig. 3(b) has one indium atom on top of an Au trimer with other indium atom among the Au trimers. In Fig. 3(f), the band crossing of  $S_2$  and  $S_3$  at the  $M$  point is reproduced, but the band  $S_1$  dispersing upward at the  $\Gamma$  point does not as shown in our calculation. The third model shown in Fig. 3(c) contains two indium atoms are on top of the Si atoms, where we note that its corresponding band structure in Fig. 3(g) does not match the experimental result either. Furthermore, the fourth model in Fig. 3(d) has one indium atom residing on top of the Au trimer while the other indium atoms sit on top of a Si atom. Its band structure, plotted in Fig. 3(h), also shows the band crossing of  $S_2$  and  $S_3$  at the  $M$  point. However, an additional band dispersing at the  $\Gamma$  point which emerges from our calculation is not seen in the experimental result.

The In coverage was further increased to  $1$  ML. Numerous models were examined, and two low-energy models are listed in the Table I. The first model CHCT-2T4-1AT has one additional In atom that is adsorbed on top of an Au trimer. The second model CHCT-3AS has all three In atoms sit on top of the Si atoms. We found that the band structures of these two models are not in agreement with experiments.<sup>48</sup>

The inclusions of SOC in the band calculations showed that the SOC mainly causes the splitting of surface bands that the Au atoms contribute to. We further notice that for the models to match the experimental dispersions of bands  $S_1$ ,  $S_2$ , and  $S_3$  where their  $E_{\text{shift}}$  are provided in Table I, the band gaps of  $S_2$  and  $S_3$  at the  $M$  point have to be less than  $0.354$  eV. Considerations of spin-orbit coupling in these systems showed that the splittings of the  $S_2$  and  $S_3$  bands leave gaps near the  $M$  point that are smaller and close to the experimental resolution limit of  $0.1$  eV. Finally, the splittings of the  $S_1$  and  $S_3$  bands around the  $M$  point are found to be Rashba spin-orbit

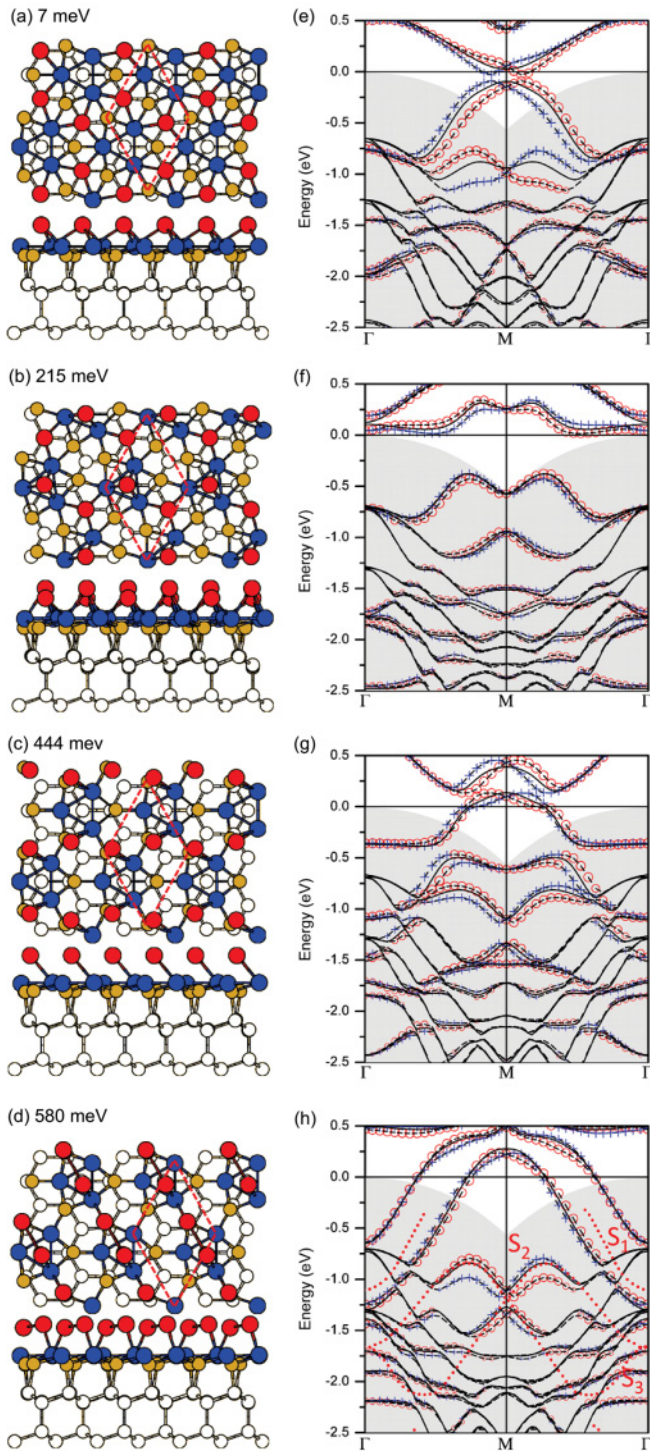


FIG. 3. (Color online) (a), (b), (c), and (d) show models for two In atoms adsorbed on  $\sqrt{3}$  at In coverage of 2/3 ML, and (e), (f), (g), and (h) are their corresponding band structures along  $\Gamma$ -M- $\Gamma$ .

splitting<sup>57</sup> since the In-Au-Si surface layer formed a potential gradient at the surface.

After investigating the models at different In coverages, we further discuss the stability as a function of In coverage. The relative surface energies of the models versus In coverage are plotted in Fig. 4(a). The plot shows that the system at In coverage of 1/3 ML is most stable, while the experimental

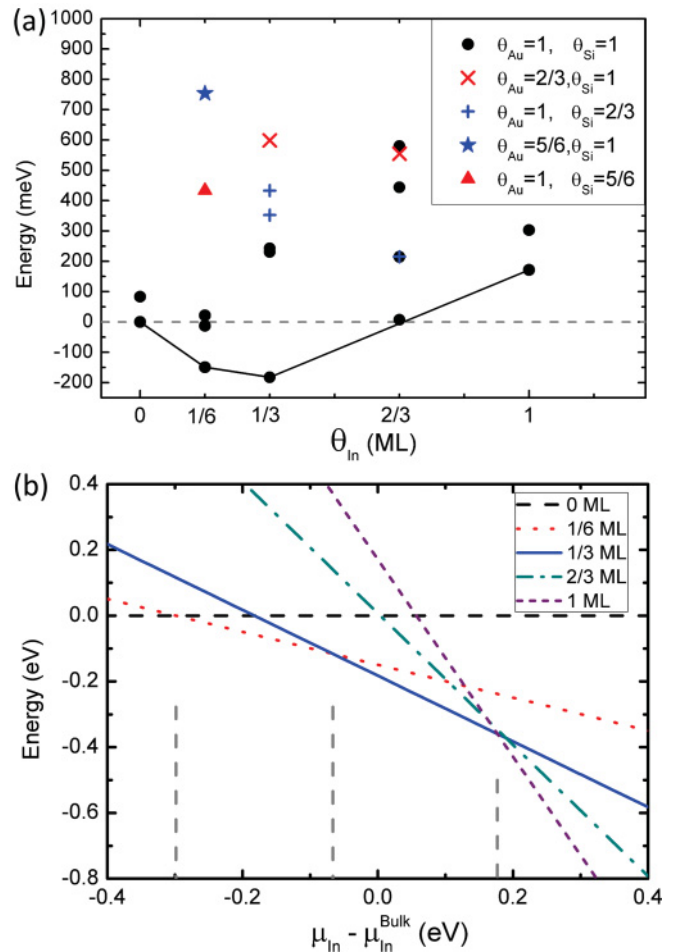


FIG. 4. (Color online) (a) The relative surface energies of models vs In coverage. (b) The relative surface energies (meV per  $\sqrt{3}$  cell) of lowest-energy models at different In coverages vs the chemical potential of In.

observations suggested rather that the In coverage is 1/6 ML.<sup>46,48</sup> The lines connecting the lowest-energy models form a convex hull, implying the surface is less stable at In coverage of 2/3 ML. Moreover, a consistent trend was found. The lowest-energy models at coverages ranging from 1/6 to 1 ML are those of In atoms sitting on the T4 sites.

Next, we discuss the stability as a function of the chemical potential. The relative surface energies of the lowest-energy models versus the chemical potential of In are plotted in Fig. 4. A quick inspection of Fig. 4 reveals that for  $(\mu_{\text{In}} - \mu_{\text{In}}^{\text{bulk}}) > 0.177$  eV the most stable structure is the model at In coverage of 1 ML. Gradually, when  $-0.066$  eV  $< (\mu_{\text{In}} - \mu_{\text{In}}^{\text{bulk}}) < 0.177$  eV the model at In coverage of 1/3 ML exhibits the most stability. The bulk energy of In is within this range. However, when  $-0.299$  eV  $< (\mu_{\text{In}} - \mu_{\text{In}}^{\text{bulk}}) < -0.066$  eV, the most stable structure is the model at In coverage of 1/6 ML. We note that when the chemical potential differs from the bulk value by only  $-0.066$  eV the model at In coverage of 1/6 ML has a lower energy than the model at In coverage of 1/3 ML. When  $(\mu_{\text{In}} - \mu_{\text{In}}^{\text{bulk}}) < -0.299$  eV, the surface exhibits the most stability without any In adsorption. The lowest-energy model at 2/3 ML seems to be less stable with respect to the chemical potential.

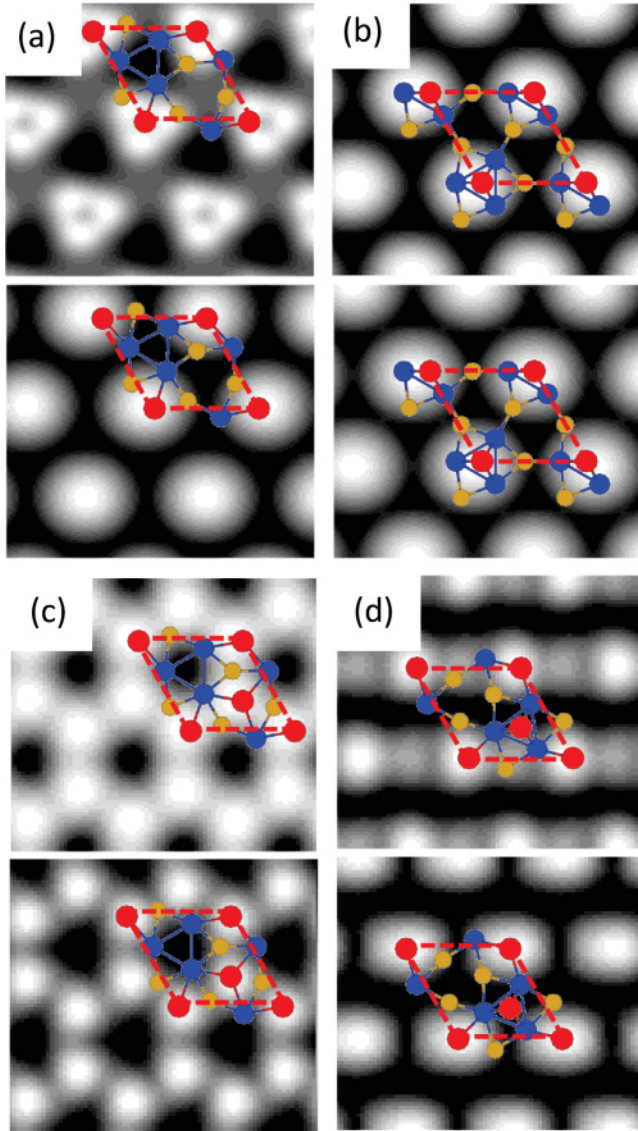


FIG. 5. (Color online) The empty-state (top) and filled-state (bottom) images of the (a) CHCT-T4 [Fig. 1(c)] and (b) CHCT-AT [Fig. 1(d)] models at 1/3 ML. (c) and (d) are those of CHCT-2T4 [Fig. 3(a)] and CHCT-T4-AS [Fig. 3(b)]. The sample biases are +1.0 V and  $-1.0$  V for empty (top) and filled (bottom) states, respectively.

Finally, we calculated STM images of our models and compared them with the experimental observations.<sup>46</sup> In Figs. 5(a) and 5(b), our simulated STM images of 1/3-ML models show one bright spot per  $\sqrt{3}$  cell and thus do not exhibit the hexagonal pattern. Furthermore, the simulated STM images of the lowest-energy model of 2/3 ML as shown in Fig. 5(c) exhibit the hexagonal pattern, which matches the experiment STM observations. However, the STM experiment was performed at a low coverage of 0.15 ML (around 1/6 ML)

and at room temperature (300 K). A plausible explanation for this discrepancy was proposed by Gruznev *et al.*<sup>46</sup> in which the In atoms migrate actively and hop among neighboring T4 sites at 300 K and the STM observations in fact were taken as the time-averaging images. Their further measurement at a lower temperature (125 K) verified one protrusion per  $\sqrt{3}$  cell, meaning that one In atom sits on one  $\sqrt{3}$  cell. In addition, the ARPES study by Kim *et al.*<sup>48</sup> was performed at a temperature ranging from 300 K down to 40 K, and the surface band dispersions have no significant change. Moreover, our calculations showed a huge change in the band dispersions at indium coverage of 2/3 ML. Based on these facts, we can conclude that at 1/6 ML, even though In atoms are active at the surface at 300 K, only one indium is within one  $\sqrt{3}$  cell at any time; thus the band dispersion measurement<sup>48</sup> should be a mixture of dispersions from the CHCT and CHCT-T4 models, while at a lower temperature, the indium atoms will be frozen,<sup>46</sup> and thus the same mixture of dispersions is expected. Further experimental study at a higher coverage is needed due to the interesting surface band dispersions at 2/3 ML. Using the  $\sqrt{3}$  as a template, exotic band dispersions may be tailored by adsorbing different metals.

#### IV. CONCLUSIONS

In conclusion, atomic and electronic structures of the In-adsorbed Au/Si(111)- $\sqrt{3} \times \sqrt{3}$  surface reconstruction were examined using first-principles calculations at In coverages ranging from 1/6 to 1 ML. The analysis of stability due to the chemical potential indicates that the model at In coverage of 2/3 ML is less stable. The T4 site was found to be the preferred adsorption site for indium atoms. The band structures of the numerous models were analyzed in detail. Our results show that the calculated bands for lowest-energy model at In coverage of 1/3 ML are in fair agreement with the identified bands in the angle-resolved photoemission study. Finally, the surface bands around the  $M$  point exhibit Rashba spin-orbit splitting since the In-Au-Si layer formed a potential gradient at the surface.

#### ACKNOWLEDGMENTS

F.C.C. was supported by the National Center of Theoretical Sciences (NCTS) and the National Science Council of Taiwan under Grant No. NSC98-2112-M110-002-MY3. F.C.C. is also grateful to the National Center for High-performance Computing for computer time and facilities. V.O. was supported as part of the Molecularly Engineered Energy Materials (MEEM), an Energy Frontier Research Center funded by the US Department of Energy, Office of Science, Office of Basic Energy Sciences, under Award No. DE-SC0001342. We thank Steven C. Erwin at the Naval Research Laboratory for very helpful discussions.

\*fchuang@mail.nsysu.edu.tw

<sup>1</sup>K. Oura, M. Katayama, F. Shoji, and T. Hanawa, *Phys. Rev. Lett.* **55**, 1486 (1985).

<sup>2</sup>J. M. Nicholls, F. Salvan, and B. Reihl, *Phys. Rev. B* **34**, 2945 (1986).

<sup>3</sup>J. H. Huang and R. S. Williams, *Phys. Rev. B* **38**, 4022 (1988).

<sup>4</sup>Ph. Dumas, A. Humbert, G. Mathieu, P. Mathiez, C. Mouttet, R. Rolland, F. Salvan, and F. Thibaudau, *J. Vac. Sci. Technol. A* **6**, 517 (1988).

- <sup>5</sup>L. E. Berman, B. W. Batterman, and J. M. Blakely, *Phys. Rev. B* **38**, 5397 (1988).
- <sup>6</sup>J. Nogami, A. A. Baski, and C. F. Quate, *Phys. Rev. Lett.* **65**, 1611 (1990).
- <sup>7</sup>C. J. Karlsson, E. Landemark, L. S. O. Johansson, and R. I. G. Uhrberg, *Phys. Rev. B* **42**, 9546 (1990).
- <sup>8</sup>M. Chester and T. Gustafsson, *Surf. Sci.* **256**, 135 (1991).
- <sup>9</sup>J. Quinn, F. Jona, and P. M. Marcus, *Phys. Rev. B* **46**, 7288 (1992).
- <sup>10</sup>Y. G. Ding, C. T. Chan, and K. M. Ho, *Surf. Sci.* **275**, L691 (1992).
- <sup>11</sup>S. Hasegawa, Y. Nagai, T. Oonishi, and S. Ino, *Phys. Rev. B* **47**, 9903 (1993).
- <sup>12</sup>I. H. Hong, D. K. Liao, Y. C. Chou, C. M. Wei, and S. Y. Tong, *Phys. Rev. B* **54**, 4762 (1996).
- <sup>13</sup>Y. Nakajima, C. Voges, T. Nagao, S. Hasegawa, G. Klos, and P. Pfnur, *Phys. Rev. B* **55**, 8129 (1997).
- <sup>14</sup>T. Okuda, H. Daimon, S. Suga, Y. Tezuka, and S. Ino, *Appl. Surf. Sci.* **121–122**, 89 (1997).
- <sup>15</sup>A. Saito, K. Izumi, T. Takahashi, and S. Kikuta, *Phys. Rev. B* **58**, 3541 (1998).
- <sup>16</sup>T. Nagao, S. Hasegawa, K. Tsuchie, S. Ino, C. Voges, G. Klos, H. Pfnur, and M. Henzler, *Phys. Rev. B* **57**, 10100 (1998).
- <sup>17</sup>E. A. Khramtsova, H. Sakai, K. Hayashi, and A. Ichimiya, *Surf. Sci.* **433–435**, 405 (1999).
- <sup>18</sup>K. N. Altmann, J. N. Crain, A. Kirakosian, J. L. Lin, D. Y. Petrovykh, F. J. Himpsel, and R. Losio, *Phys. Rev.* **64**, 035406 (2001).
- <sup>19</sup>H. M. Zhang, T. Balasubramanian, and R. I. G. Uhrberg, *Phys. Rev. B* **66**, 165402 (2002).
- <sup>20</sup>J. N. Crain, K. N. Altmann, C. Bromberger, and F. J. Himpsel, *Phys. Rev. B* **66**, 205302 (2002).
- <sup>21</sup>T. Kadohira, J. Nakamura, and S. Watanabe, *e-J. Surf. Sci. Nanotechnol.* **2**, 146 (2004).
- <sup>22</sup>H. W. Kim, K. S. Shin, J. R. Ahn, and J. W. Chung, *J. Korean Phys. Soc.* **35**, S534 (1999).
- <sup>23</sup>R. Losio, K. N. Altmann, and F. J. Himpsel, *Phys. Rev. Lett.* **85**, 808 (2000).
- <sup>24</sup>C. Seifert, R. Hild, M. H. Hoegen, R. A. Zhachuk, and B. Z. Olshanetsky, *Surf. Sci.* **488**, 233 (2001).
- <sup>25</sup>T. Hasegawa, K. Takata, S. Hosaka, and S. Hosoki, *J. Vac. Sci. Technol. A* **8**, 241 (1990).
- <sup>26</sup>A. A. Baski, J. Nogami, and C. F. Quate, *Phys. Rev. B* **41**, 10247 (1990).
- <sup>27</sup>J. D. O'Mahony, J. F. McGilp, C. F. J. Flipse, P. Weightman, and F. M. Leibsle, *Phys. Rev. B* **49**, 2527 (1994).
- <sup>28</sup>L. D. Marks and R. Plass, *Phys. Rev. Lett.* **75**, 2172 (1995).
- <sup>29</sup>T. Hasegawa, S. Hosaka, and S. Hosoki, *Surf. Sci.* **357**, 858 (1996).
- <sup>30</sup>S. C. Erwin, *Phys. Rev. Lett.* **91**, 206101 (2003).
- <sup>31</sup>M. H. Kang and J. Y. Lee, *Surf. Sci.* **531**, 1 (2003).
- <sup>32</sup>A. Kirakosian, R. Bennewitz, F. J. Himpsel, and L. W. Bruch, *Phys. Rev. B* **67**, 205412 (2003).
- <sup>33</sup>H. S. Yoon, S. J. Park, J. E. Lee, C. N. Whang, and I. W. Lyo, *Phys. Rev. Lett.* **92**, 096801 (2004).
- <sup>34</sup>J. L. McChesney, J. N. Crain, V. Perez-Dieste, Fan Zheng, M. C. Gallagher, M. Bissen, C. Gundelach, and F. J. Himpsel, *Phys. Rev. B* **70**, 195430 (2004).
- <sup>35</sup>H. S. Yoon, J. E. Lee, S. J. Park, I. W. Lyo, and M. H. Kang, *Phys. Rev. B* **72**, 155443 (2005).
- <sup>36</sup>S. Riikonen and D. Sanchez-Portal, *Phys. Rev. B* **71**, 235423 (2005).
- <sup>37</sup>C. Y. Ren, S. F. Tsay, and F. C. Chuang, *Phys. Rev. B* **76**, 075414 (2007).
- <sup>38</sup>F. C. Chuang, C. H. Hsu, C. Z. Wang, and K. M. Ho, *Phys. Rev. B* **77**, 153409 (2008).
- <sup>39</sup>S. C. Erwin, I. Barke, and F. J. Himpsel, *Phys. Rev. B* **80**, 155409 (2009).
- <sup>40</sup>W. H. Choi, H. Koh, E. Rotenberg, and H. W. Yeom, *Phys. Rev. B* **75**, 075329 (2007).
- <sup>41</sup>C. H. Hsu, F. C. Chuang, M. A. Albao, and V. Yeh, *Phys. Rev. B* **81**, 033407 (2010).
- <sup>42</sup>K. S. Kim, S. C. Jung, M. H. Kang, and H. W. Yeom, *Phys. Rev. Lett.* **104**, 246803 (2010).
- <sup>43</sup>S. C. Jung, and M. H. Kang, *Surf. Sci.* **605**, 551 (2011).
- <sup>44</sup>Y. G. Ding, C. T. Chan, and K. M. Ho, *Phys. Rev. Lett.* **67**, 1454 (1991).
- <sup>45</sup>J. Y. Lee and M. H. Kang, *J. Korean Phys. Soc.* **53**, 3671 (2008).
- <sup>46</sup>D. V. Gruznev, I. N. Filippov, D. A. Olyanich, D. N. Chubenko, I. A. Kuyanov, A. A. Saranin, A. V. Zotov, and V. G. Lifshits, *Phys. Rev. B* **73**, 115335 (2006).
- <sup>47</sup>D. V. Gruznev, A. V. Matetskiy, L. V. Bondarenko, E. A. Borisenko, D. A. Tsukanov, A. V. Zotov, and A. A. Saranin, *Surf. Sci.* **605**, 1420 (2011).
- <sup>48</sup>J. K. Kim, K. S. Kim, J. L. McChesney, E. Rotenberg, H. N. Hwang, C. C. Hwang, and H. W. Yeom, *Phys. Rev. B* **80**, 075312 (2009).
- <sup>49</sup>Y. Ohtsubo, S. Hatta, K. Yaji, H. Okuyama, K. Miyamoto, T. Okuda, A. Kimura, H. Namatame, M. Taniguchi, and T. Aruga, *Phys. Rev. B* **82**, 201307 (2010).
- <sup>50</sup>A. Takayama, T. Sato, S. Souma, and T. Takahashi, *Phys. Rev. Lett.* **106**, 166401 (2011).
- <sup>51</sup>E. Frantzeskakis, S. Pons, and M. Grioni, *Phys. Rev. B* **82**, 085440 (2010).
- <sup>52</sup>I. Gierz, T. Suzuki, E. Frantzeskakis, S. Pons, S. Ostanin, A. Ernst, J. Henk, M. Grioni, K. Kern, and C. R. Ast, *Phys. Rev. Lett.* **103**, 046803 (2009).
- <sup>53</sup>J. P. Perdew, K. Burke, and M. Ernzerhof, *Phys. Rev. Lett.* **77**, 3865 (1996).
- <sup>54</sup>P. Hohenberg and W. Kohn, *Phys. Rev.* **136**, B864 (1964); W. Kohn and L. J. Sham, *ibid.* **140**, A1135 (1965).
- <sup>55</sup>G. Kresse and D. Joubert, *Phys. Rev. B* **59**, 1758 (1999).
- <sup>56</sup>G. Kresse and J. Hafner, *Phys. Rev. B* **47**, 558 (1993); G. Kresse and J. Furthmuller, *ibid.* **54**, 11 169 (1996).
- <sup>57</sup>Y. A. Bychkov and E. I. Rashba, *JETP Lett.* **39**, 78 (1984).